

Constraint-based Cooperative Control of Multiple Aerial Manipulators for Handling an Unknown Payload

Hyeonbeom Lee and H. Jin Kim, *Member, IEEE*

Abstract—This paper presents the planning and control synthesis of cooperative aerial manipulators to carry an unknown object together. The on-line parameter estimation algorithm is designed to estimate the unknown physical parameters of the common payload such as mass and moment of inertia, without the need of multi-axis force/torque sensors. Based on the augmented adaptive sliding mode controller with the estimated physical parameters, the desired trajectory of each aerial manipulator is generated to track the desired trajectory of corresponding end effector. In order to carry an unknown object safely considering the actuation limit of the hexacopter, we use the task priority to satisfy the unilateral constraints determined by the allowable flight envelope. To validate our approach, the experimental result on a successful transportation by using multiple custom-made aerial manipulators is shown. This result suggests that the proposed approach can be utilized for safe cooperative aerial transportation.

Index Terms—Cooperative manipulation, aerial robots, motion planning, multiple tasks, consensus.

I. INTRODUCTION

AFFORDABILITY and simple hardware structure of multirotors have promoted the rapidly growing interests as an easy-to-work-with platform [1]. Cooperative aerial transportation, which is one of key potential applications of multirotors, is aimed at transporting a heavier or bulkier object that cannot be handled by a single vehicle [2]–[8]. However, cooperations involves complexity associated with multiple robots in comparison with a single robot such as coordination, synchronization of manipulators or stability due to the actuation limits. In addition, force/torque sensors can be often used to estimate the unknown physical parameters of an object [9,10], but availability of these sensors in small aerial robots could be limited because multi-axis force/torque sensors are often heavy and expensive.

This paper is interested in resolving these problems for cooperative aerial manipulators. To achieve this goal, we concentrate on two tasks: 1) estimation and control of cooperative aerial robots and 2) safe planning within the flight envelope. First, unknown physical properties of a payload are estimated without force/torque sensors and used in controller design to follow the desired trajectory. Second, the planning algorithm is proposed to efficiently generate the desired path of each aerial

Manuscript received September 06, 2016; revised March 11, 2017; accepted March 19, 2017. This research was supported in part by the Program of Development of Space Core Technology under grant NRF-2014M1A3A3A02034854 and in part by the Framework of International Cooperation Program under Grant NRF-2014R1A2A1A12067588 through the National Research Foundation of Korea funded by the Ministry of Science, ICT and Future Planning. (*Corresponding author: H. Jin Kim*)

The authors are with the Automation and Systems Research Institute, Department of Mechanical and Aerospace Engineering, Seoul National University, Seoul, Korea. (e-mail: h.beom.lee@gmail.com, hjinkim@snu.ac.kr)

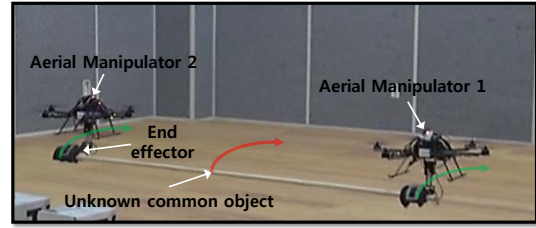


Fig. 1. Two aerial manipulators, each consisting of hexacopters and a robotic arm, transport an unknown common object.

manipulator. By using this algorithm, the end effectors remain in the allowable flight region where the aerial manipulators can avoid the excess of actuation limits.

A. Contribution

The contributions of this paper can be summarized as follows: first, we address an on-line parameter estimator and a controller to handle an unknown common payload without using the force/torque sensors. In this paper, we develop the estimation algorithm for multiple robots by exploiting the decoupled dynamics and consensus. Unlike the research in [11] for a single aerial manipulator with point mass of a payload, our estimation and control algorithm can handle a payload with unknown inertia and are not limited by the number of robots. In addition, we improve the estimation performance of multiple robots by sharing the estimated physical parameters of the payload. Second, we propose a real-time motion generation algorithm to transport the payload. The desired path for each end effector is generated based on the geometry of the payload, also known as kinematic coordination. The desired trajectory for each aerial manipulator in joint space is computed to satisfy the safe flight envelope by considering the capability of the aerial manipulator in real time. By exploiting unilateral constraints in task priority as described in [12,13], the allowable flight boundary is not violated during transportation without using additional optimization approaches. Finally, we validate our algorithm on custom-made aerial manipulators with two types of unknown payloads. The experimental result shows feasibility of the proposed algorithm in jointly carrying an unknown payload.

B. Related Work

Cooperative manipulation can be applied to a wide range of applications in construction sites, production lines or various remote operations. Many researchers try to achieve this goal by using ground manipulators [14,15] or aerial robots [4,5,7]. In [14], a hybrid position and force controller based on the

centralized multi-fingered dynamics was presented. In [15], they solved a suboptimal LQR-like control iteratively for cooperative manipulators transporting an object in a centralized manner. For multiple quadrotors with a gripper, in [4], they designed a centralized controller to stabilize a payload along three-dimensional trajectories in a centralized manner. Unlike fully centralized approaches, to facilitate the faster local feedback in each robot, each end effector controller was run locally while the optimization for task planning was done centrally. [5,7,15]. For aerial robots, in [5], they showed control and planning of multiple aerial robots transporting a payload via cables. The feasible solution for an equilibrium of a payload was numerically determined for the special case of a triangular payload. For aerial manipulators, a hierarchical control framework for multiple quadrotors with a 2-DoF robotic arm was simulated in [7]. In this method, cooperative force distribution among the end effectors was computed by solving constrained quadratic optimization problem. The constrained optimization [5,7] may need a relatively higher computational and communicational load.

Unlike the optimization approach, task-oriented formulation with a kinematic control does not require numerical methods [16,17]. Based on the kinematic control, a two-layer framework, in which the first layer computes the motion reference of the end effectors and the second layer calculates joint motion of the corresponding manipulator, was proposed for a ground mobile manipulator with a dual arm [9]. For cooperative quadrotor manipulators, an impedance control architecture with the two-layer framework was simulated to handle the contact forces at the end effectors [2]. However, these methods [2,9] depend on multi-axis force/torque sensors to estimate and carry an unknown common object, while our proposed algorithm does not.

In order to avoid these practical difficulties associated with force/torque sensing, a coordinated motion control based on leader-follower structure was designed for two mobile manipulators [18]. For aerial manipulators, the desired trajectories for multiple aerial manipulators were obtained by using RRT* (Rapidly exploring Random Tree star) [6,8]. In [6], the effect of a common object was compensated based on the closed-chain dynamics in joint space. However, these methods [6,8,18] require exact knowledge of a common object.

Research on handling uncertainty such as an unknown payload has begun with early work on single manipulator [19]–[21]. For cooperative manipulators, there was research for handling an inaccurate kinematic model of an object such as inaccurate orientation and length at gripping points [22,23], but they assumed that physical parameters of the object such as mass or moment of inertia were known. In [24], the physical parameters of a common object and robots arms were estimated based on a distributed adaptive coordinated control method. Furthermore, consensus algorithm for an agreement on certain quantities of group interest was also studied to handle the uncertainty in [25] or synchronization of networked mobile manipulators [26]. For multiple ground mobile manipulators, in [10], consensus for the estimation of kinematic and inertial parameters of an unknown common object was simulated by receiving the measurements of velocity and the

contact force applied to the object. However, unlike these algorithms applied to ground manipulators [10,24]–[26], aerial manipulators need to consider the actuation limit also, for the safety of aerial robots.

The transportation capability of an aerial manipulator is a crucial factor in carrying a heavy load safely. In order to determine such capability of cooperative aerial manipulators, we should deal with the problems of uncertain parameters and actuation limits simultaneously, which is difficult because of the interactions between robots. Although the least-square method to estimate unknown mass attached under a multirotor [27] or robust control for parameter uncertainty of a multirotor [28] was proposed, actuation limits of aerial robots still remain a problem. The effect of a dynamic load in a single helicopter with a gripper is considered in [29], but they do not take account of actuation limits. To avoid this issue and to operate the robots safely, in [30,31], they obtained the desired paths between a predefined initial and final configuration of a quadrotor were generated by using quadratic programming solver with constraints such as joint limits. In [32], the trajectory planning with dynamic programming was presented for a single ground mobile manipulator to satisfy the maximum carrying capacity. However, since these algorithms solve numerical optimization problems of a single robot, complexity between multiple robots cannot be dealt with in real time. In our work, the trajectories of the end effector are adjusted to satisfy the allowable flight envelope by exploiting on-line cooperative parameter estimation, which does not involve on numerical optimization.

Organization: This paper is structured as follows: background materials including task priorities and the dynamics of multiple aerial manipulators handling a common object are described in section II. The estimation and control algorithms are designed in section III. Path planning is addressed in section IV. Section V presents the experimental result. Section VI contains concluding remarks.

II. BACKGROUND

In this section, we present the necessary background for dynamics of aerial manipulators and task priority.

A. Decoupled Dynamics for Multiple Aerial Manipulators

For an aerial manipulator with n -DoF robotic arm, the coordinated frames $\Sigma_I, \Sigma_b, \Sigma_c$ represent the inertial frame, the body frame of the hexacopter and the body frame of the end effector, respectively as shown in Fig. 2. Σ_o means the body frame of the object. For the i -th manipulator, using the position of center of mass of the hexacopter in the inertial frame $\mathbf{p}_{b,i} = [x_{b,i}, y_{b,i}, z_{b,i}]^T$, Euler angles of the hexacopter $\Phi_i = [\phi_i, \theta_i, \psi_i]^T$ and joint angles of the manipulator $\eta_i = [\eta_{i,1}, \dots, \eta_{i,n}]^T$, the kinematic model can be described based on the following system state,

$$\mathbf{q}_i = \begin{bmatrix} \mathbf{p}_{b,i}^T & \Phi_i^T & \eta_i^T \end{bmatrix}^T, \quad (1)$$

for $i = 1, \dots, N_m$, where N_m is the total number of aerial manipulators. Although we use two aerial manipulators in

experiments, the proposed algorithm can be easily extended to multiple aerial manipulators. In general, we will use bold letters (e.g., \mathbf{q}_i , Φ_i) to indicate vector quantities.

When the aerial manipulator and the object interact, the resulting force $\lambda_i \in \mathbb{R}^6$ is exerted at the end effector in Σ_c of the i -th aerial manipulator. In this case, the dynamics of aerial manipulator is different from the single aerial manipulator alone. Considering the resulting force λ_i and the state \mathbf{q}_i , the equation of motion of the i -th aerial manipulator can be represented as

$$M_i(\mathbf{q}_i)\ddot{\mathbf{q}}_i + Q_i(\mathbf{q}_i, \dot{\mathbf{q}}_i)\dot{\mathbf{q}}_i + W_i(\mathbf{q}_i) = \boldsymbol{\tau}_i - J_i^T(\mathbf{q}_i)\boldsymbol{\lambda}_i, \quad (2)$$

where the control input $\boldsymbol{\tau}_i \in \mathbb{R}^{(6+n)}$ consists of inputs for 6-DoF aerial robot and n -DoF robotic arm, $M_i(\mathbf{q}_i) \in \mathbb{R}^{(6+n) \times (6+n)}$ is the inertia matrix, $Q_i(\mathbf{q}_i, \dot{\mathbf{q}}_i) \in \mathbb{R}^{(6+n) \times (6+n)}$ is the Coriolis matrix, $W_i(\mathbf{q}_i) \in \mathbb{R}^{(6+n)}$ is the gravity effect at each joint, and $J_i(\mathbf{q}_i) \in \mathbb{R}^{6 \times (6+n)}$ means the Jacobian matrix from $\Sigma_{b,i}$ to $\Sigma_{c,i}$.

To obtain the dynamics of the rigid object, we define the twist $\dot{\mathbf{q}}_o = [\mathbf{p}_o^T, \boldsymbol{\omega}_o^T]^T \in se(3)$ as a six-dimensional vector composed of translational velocity $\dot{\mathbf{p}}_o \in \mathbb{R}^3$ and rotational velocity of the object $\boldsymbol{\omega}_o \in \mathbb{R}^3$ in Σ_I .

Using $H_o = \text{diag}(m_o I_3, J_o)$ with the mass of object m_o and inertia J_o , the dynamics of rigid object can be written:

$$H_o \ddot{\mathbf{q}}_o + \mu_o \dot{\mathbf{q}}_o + G_o = \sum_{i=1}^{N_m} E_i \boldsymbol{\lambda}_i, \quad (3)$$

where μ_o and G_o can be written as

$$\mu_o = \begin{bmatrix} 0_3 & 0_3 \\ 0_3 & S(\boldsymbol{\omega}_o)J_o \end{bmatrix}, \quad G_o = \begin{bmatrix} -m_o g \mathbf{e}_3 \\ \mathbf{0}_{3 \times 1} \end{bmatrix}.$$

Here, $\mathbf{e}_3 = [0, 0, 1]^T$, $S(*)$ denotes the skew symmetric matrix, I_3 and 0_3 are 3×3 identity and zero matrices, respectively. Since E_i is the grasp matrix that can be expressed as

$$E_i = \begin{bmatrix} I_3 & 0_3 \\ S(\mathbf{r}_i) & I_3 \end{bmatrix}, \quad (4)$$

the term $\sum_{i=1}^{N_m} E_i \boldsymbol{\lambda}_i$ denotes the effective wrench acting on the common object [9] and $\mathbf{r}_i \in \mathbb{R}^3$ is a vector from the coordinated frame located at the center of the object, Σ_o , to $\Sigma_{c,i}$.

In our configuration, with the assumption of rigid grasping, all positions and orientations of the common object and the end-effectors coordinates can be expressed relative to a common reference frame. From the relationship between \mathbf{q}_i and \mathbf{q}_o (i.e., $\dot{\mathbf{q}}_o = E_i^{-T} J_i \dot{\mathbf{q}}_i$), the equation of motion of the i -th aerial manipulator with the object can be obtained as:

$$D_i(\mathbf{q}_i)\ddot{\mathbf{q}}_i + C_i(\mathbf{q}_i, \dot{\mathbf{q}}_i)\dot{\mathbf{q}}_i + G_i(\mathbf{q}_i) = \boldsymbol{\tau}_i, \quad (5)$$

Here, the matrices are computed as

$$\begin{aligned} D_i &= M_i(\mathbf{q}_i) + c_i M_o(\mathbf{q}_i), \quad G_i = W_i + c_i W_o(\mathbf{q}_i) \\ C_i &= Q_i(\mathbf{q}_i, \dot{\mathbf{q}}_i) + c_i Q_o(\mathbf{q}_i, \dot{\mathbf{q}}_i) + c_i J_i^T(E_i^T H_o E_i^{-T}) \dot{J}_i. \end{aligned}$$

where the following representation can be taken from the results in [6] as $M_o(\mathbf{q}_i) = J_i^T(E_i^T H_o E_i^{-T}) J_i$, $Q_o(\mathbf{q}_i, \dot{\mathbf{q}}_i) =$

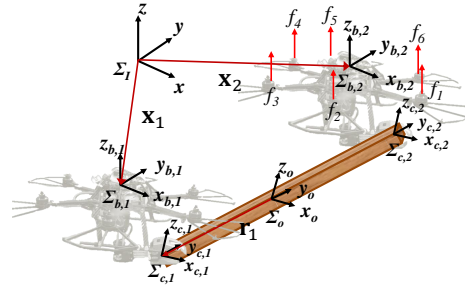


Fig. 2. Two cooperative multirotors manipulate a common object.

$J_i^T(E_i^\dagger \mu_o E_i^{-T}) J_i$, $W_o(\mathbf{q}_i) = J_i^T E_i^\dagger G_o$. E_i^\dagger can be obtained by the Moore-Penrose pseudo-inverse in [33] as

$$c_i E_i^\dagger = \begin{bmatrix} c_i I_3 & -c_i S(\mathbf{r}_i) \Pi^{-1} \\ 0_3 & c_i \Pi^{-1} \end{bmatrix}, \quad (6)$$

where c_i is a constant weight such that $\sum_{i=1}^{N_m} c_i = 1$ and $\Pi = I_3 + \sum_{i=1}^{N_m} c_i S(\mathbf{r}_i) S^T(\mathbf{r}_i)$.

B. Desired Roll and Pitch of the Hexacopter

In order to operate the hexacopter, the computed control signal $\boldsymbol{\tau}_i = [\tau_i(1), \dots, \tau_i(6+n)]^T$ should be converted to motor control command (See [34] for more detail). To do so, the first two elements of $\boldsymbol{\tau}_i$, i.e., $\tau_i(1)$ and $\tau_i(2)$, are used to generate the desired roll ϕ_i^d and pitch angle θ_i^d for the i -th aerial manipulator. These values can be computed by the following rule:

$$\begin{bmatrix} \phi_i^d \\ \theta_i^d \end{bmatrix} = \frac{1}{\tau_i(3)} \begin{bmatrix} \cos(\psi_i) & \sin(\psi_i) \\ \sin(\psi_i) & -\cos(\psi_i) \end{bmatrix} \begin{bmatrix} \tau_i(1) \\ \tau_i(2) \end{bmatrix}. \quad (7)$$

Because the desired roll ϕ_i^d and pitch θ_i^d are automatically generated by the control input of x and y direction according to (7), the desired trajectory of each aerial manipulator is given as $[x_i^d, y_i^d, z_i^d, \psi_i^d, \eta_{i,1}^d, \dots, \eta_{i,n}^d]$. Here, the superscript d means the desired value and i means the i -th aerial manipulator. The more detailed explanation is covered in Sec. IV.

C. Task Priority

We employ the formulation of task priority [35,36] to generate trajectories satisfying unilateral constraints or maintaining the safety envelope of the end effector, which are referred to as tasks. The description in this section is based on [35,36], and the details can be found therein.

Consider the k -th task for the i -th aerial manipulator with the differential kinematic equation:

$$\dot{\gamma}_{i,k} = T_{i,k} \dot{\nu}_{i,k}, \quad i = 1, \dots, N_m \quad (8)$$

where $\gamma_{i,k} \in \mathbb{R}^{m_{i,k}}$ is the task vector representing the Cartesian coordinate of the end effector for the task k and $\nu_{i,k} = [\mathbf{p}_{b,i}^T, \boldsymbol{\eta}_i^T]^T \in \mathbb{R}^{(3+n)}$ is the vector consisting of the position and joint angles of the aerial manipulator. $T_{i,k}$ is the transformation matrix between $\dot{\nu}_{i,k}$ and $\dot{\gamma}_{i,k}$. Note that the dimension of the vector $\dot{\gamma}_{i,k}$ can vary depending on the specific task defined by user.

From [35], we can obtain the following relation as:

$$\dot{\nu}_{i,k} = T_{i,k}^\dagger \dot{\gamma}_{i,k} + P \dot{\nu}_{i,k}^N = \dot{\nu}_{i,k}^N + T_{i,k}^\dagger (\dot{\gamma}_{i,k} - T_{i,k} \dot{\nu}_{i,k}^N),$$

where \dagger is the pseudo-inverse, $P = I_{(3+n)} - T_{i,k}^\dagger T_{i,k}$ is a projector in the null space of the transformation matrix and I_{3+n} is $(3+n) \times (3+n)$ identity matrix. Then, the hierarchy of multiple tasks is computed by projecting the k -th task in the null space of all the higher priority tasks as

$$\dot{\nu}_{i,k} = \dot{\nu}_{i,k-1} + (T_{i,k} P_{i,k-1}^A)^\dagger (\dot{\gamma}_{i,k} - T_{i,k} \dot{\nu}_{i,k-1}), \quad (9)$$

initialized with the zero matrix i.e., $\dot{\nu}_{i,k} = 0_{(3+n)}$. $P_{i,k}^A$ is the projector in the null space of the augmented Jacobian matrix of the k -th task as

$$T_{i,k}^A = [\begin{array}{ccc} T_{i,1} & \cdots & T_{i,k} \end{array}]^T. \quad (10)$$

Note that the projector in null space of k -th task can be calculated by using recursive expression [36] as

$$P_{i,k}^A = P_{i,k-1}^A - (T_{i,k} P_{i,k-1}^A)^\dagger T_{i,k} P_{i,k-1}^A, \quad (11)$$

initialized with the identity matrix i.e., $P_{i,0} = I_n$. Note that the pseudo-inverse of the Jacobian matrix may not exist at singularities or in their neighbourhood. To resolve this issue, we use Jacobian Damping (JD) as described in [37].

III. ESTIMATOR AND CONTROLLER DESIGN

In this section, we address the on-line parameter estimation algorithm based on the system parameterization with respect to the unknown payload. Based on the estimated parameter, the controller for each aerial manipulator is designed. The total control structure is shown in Fig. 3. The desired trajectories of the end effectors are generated by kinematic coordination. Each aerial manipulator follows its own trajectory computed by the trajectory of the corresponding end effector, while estimating the parameter of an unknown payload in real time. The estimation result is communicated to other aerial manipulator(s).

A. Parameter Estimation with System Parametrization

When the end-effector of the robotic arm grabs an unknown common object, the physical properties of the combined dynamics in (5) are changed because of the unknown mass m_o and inertia J_o . By designing the on-line parameter estimator, we let the controller compensate the unknown effects due to the unknown common object. Before achieving this goal, we first represent the combined dynamics as:

$$\begin{aligned} \hat{D}_i &= M_i + c_i J_i^T (E_i^\dagger \hat{H}_o E_i^{-T}) J_i \\ \hat{C}_i &= Q_i + c_i J_i^T (E_i^\dagger \hat{\mu}_o E_i^{-T}) J_i + c_i J_i^T (E_i^\dagger \hat{H}_o E_i^{-T}) \dot{J}_i \\ \hat{G}_i &= W_i + c_i J_i^T E_i^\dagger \hat{G}_o, \end{aligned} \quad (12)$$

where $\hat{\cdot}$ is the vector or matrix which includes the estimated parameters on the object of the i -th aerial manipulator (i.e., $\hat{m}_{o,i}$ and $\hat{J}_{o,i}$).

Before deriving the parameter estimator, let us consider the unknown parameter $\hat{J}_{o,i}$. In order to detect the unknown object, we can use the 3D CAD model of the target object as shown in [38]. After matching the unknown object to the

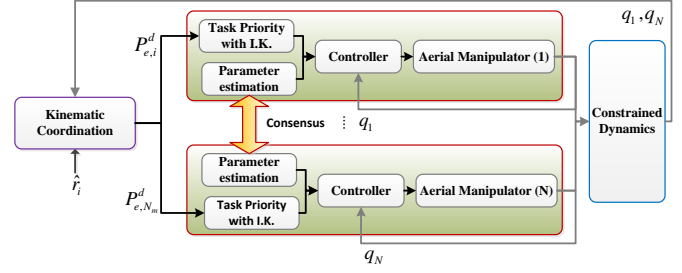


Fig. 3. Overall structure for the proposed synthesis.

CAD model, multiple aerial manipulators can detect and grasp the unknown object by using a proper vision algorithm. In this paper, we consider the scenarios after grasping the object, so this is beyond the scope of this paper. Therefore, we use the following assumption.

Assumption 1. *The geometric dimension of the common object is known.*

Based on the assumption 1, for example, the common object is a cylinder with the radius r_c and length h_c , then the unknown inertia $\hat{J}_{o,i}$ can be expressed with respect to the unknown mass $\hat{m}_{o,i}$ as:

$$\hat{J}_{o,i} = \hat{m}_{o,i} R_o \begin{bmatrix} I_{ox} & 0 & 0 \\ 0 & I_{oy} & 0 \\ 0 & 0 & I_{oz} \end{bmatrix} R_o^T, \quad (13)$$

where $I_{ox} = I_{oz} = \frac{1}{12}(3r_c^2 + h_c^2)$, $I_{oy} = \frac{1}{2}r_c^2$ and R_o is the rotation matrix of the object. Therefore, the parameterized equation in (12) can be rewritten with respect to $\hat{m}_{o,i}$ as

$$\begin{aligned} \hat{D}_i &= M_i + \hat{m}_{o,i} H_1 \\ \hat{C}_i &= Q_i + \hat{m}_{o,i} H_2 \\ \hat{G}_i &= W_i + \hat{m}_{o,i} H_3, \end{aligned} \quad (14)$$

where H_1 , H_2 and H_3 are the matrices with known physical parameters and calculated from (12). Finally, by using (14), the dynamics in (5) can be rewritten as:

$$\hat{m}_{o,i} (H_1 \ddot{\mathbf{q}}_i + H_2 \dot{\mathbf{q}}_i + H_3) = \mathbf{U}_i(t), \quad (15)$$

by introducing the forcing term including control input τ_i in

$$\mathbf{U}_i(t) = \tau_i - M_i \ddot{\mathbf{q}}_i - Q_i \dot{\mathbf{q}}_i - W_i. \quad (16)$$

Now, we design the parameter estimator based on the parameterized dynamics in (15).

$$\begin{aligned} C^* \dot{\hat{\mathbf{q}}}_i + K^* \hat{\mathbf{q}}_i + \hat{m}_{o,i} (H_1 \ddot{\mathbf{q}}_i + H_2 \dot{\mathbf{q}}_i + H_3) \\ = \mathbf{U}_i(t) + C^* \dot{\mathbf{q}}_i + K^* \mathbf{q}_i, \end{aligned} \quad (17)$$

where $C^* \in \mathbb{R}^{(6+n) \times (6+n)}$ and $K^* \in \mathbb{R}^{(6+n) \times (6+n)}$ are user-defined gain matrices and $\hat{\mathbf{q}}_i$ is the estimated state of the i -th aerial manipulator. For initial parameter update, $\hat{\mathbf{q}}_i(0) \neq \mathbf{q}_i(0)$ is recommended.

If the state estimation error is defined as $\mathbf{e}_i = \hat{\mathbf{q}}_i - \mathbf{q}_i$, then the parameter update rule for $\hat{m}_{o,i}$ can be computed as:

$$\dot{\hat{m}}_{o,i} = \Gamma_1 \mathbf{e}_i^T (H_1 \ddot{\mathbf{q}}_i + H_2 \dot{\mathbf{q}}_i + H_3) + \Gamma_2 \sum_{j=1}^{N_m} (\hat{m}_{o,j} - \hat{m}_{o,i}), \quad (18)$$

where Γ_1 and Γ_2 are the learning and consensus rates, respectively. Using (5) and (17), the error dynamics can be written as:

$$C^* \ddot{\mathbf{e}}_i + K^* \mathbf{e}_i + \tilde{D}_i \ddot{\mathbf{q}}_i + \tilde{C}_i \dot{\mathbf{q}}_i + \tilde{G}_i = 0, \quad (19)$$

where $\tilde{D}_i = \hat{D}_i - D_i$, $\tilde{C}_i = \hat{C}_i - C_i$ and $\tilde{G}_i = \hat{G}_i - G_i$.

If the controller for the aerial manipulator is designed properly (to be discussed in Sec. III-B), then the state variables will remain bounded. Then we can obtain the stable error dynamics as follows.

Lemma 1. *If the state variables \mathbf{q}_i , $\dot{\mathbf{q}}_i$ and $\ddot{\mathbf{q}}_i$ are bounded by the forcing term $\mathbf{U}_i(t)$, then the error dynamics in (19) is asymptotically stable.*

Proof. See Appendix A. \square

Here, parameter convergence, i.e., $\tilde{m}_{o,i} \rightarrow 0$, follows from [19] when the persistence of excitation is assumed.

B. Controller Design

The aerial manipulators are subject to from inevitable external uncertainties such as ground effects or downwash from other manipulators. To resolve this problem, we propose an adaptive sliding mode controller for each aerial manipulator. Let us define the control error $\mathbf{e}_{c,i} = \mathbf{q}_i - \mathbf{q}_i^d$ between the actual state \mathbf{q}_i and the desired state \mathbf{q}_i^d of the i -th aerial manipulator. Then, the sliding surface variable \mathbf{s}_i can be written as:

$$\mathbf{s}_i := \dot{\mathbf{q}}_i - \dot{\mathbf{q}}_i^d = \dot{\mathbf{e}}_{c,i} + \Lambda_i \mathbf{e}_{c,i}, \quad (20)$$

where $\dot{\mathbf{q}}_i^d = \dot{\mathbf{q}}_i^d - \Lambda_i \mathbf{e}_{c,i}$ and Λ_i is a diagonal gain matrix. Based on (20), the control input τ_i is designed as:

$$\tau_i = \hat{D}_i \ddot{\mathbf{q}}_i^r + \hat{C}_i \dot{\mathbf{q}}_i^r + \hat{G}_i - (K_s + \delta_i) \mathbf{s}_i + \xi_i^f + \hat{\Delta}_i, \quad (21)$$

where K_s is a diagonal gain matrix and $\hat{\Delta}_i$ is uncertainty estimated by the i -th aerial manipulator. The variable ξ_i^f is calculated by letting $\xi_i := C^* \ddot{\mathbf{e}}_i + K^* \mathbf{e}_i \in \mathbb{R}^{(6+n)}$ pass through a first-order filter with time constant α as:

$$\alpha \dot{\xi}_i^f + \xi_i^f = \xi_i, \quad \xi_i^f(0) = \xi_i(0). \quad (22)$$

For the stability analysis, we should check the skew-symmetric property of $\hat{D}_i - 2\hat{C}_i$ as described in [6]. With any arbitrary vector $\mathbf{s} \in \mathbb{R}^{(6+n)}$, we can observe

$$\mathbf{s}^T (\hat{D}_i - 2\hat{C}_i) \mathbf{s} = c_i \mathbf{s}^T [J_i^T E_i^\dagger (\hat{H}_o - 2\mu) E_i^{-T} J_i] \mathbf{s}. \quad (23)$$

In this case, applying the fact that $\hat{J}_o = S(\omega_o) J_o - J_o S(\omega_o)$, $\hat{H}_o - 2\mu_o$ in [9] can be rewritten as

$$(\hat{H}_o - 2\mu)^T = \begin{bmatrix} 0_3 & 0_3 \\ 0_3 & -S(\omega_o) J_o - J_o S(\omega_o) \end{bmatrix}. \quad (24)$$

Here, the term $-S(\omega_o) J_o - J_o S(\omega_o)$ in (24) can be easily computed using the angular velocity of the end effector, which is the same as ω_o due to the rigid grasping assumption. However, the term in (23) may not satisfy the skew-symmetric property since $E_i^\dagger \neq E_i^{-T}$. To overcome this issue, we define the auxiliary control input δ_i as:

$$\delta_i := \frac{c_i}{2} J_i^T E_i^\dagger (\hat{H}_o - 2\hat{\mu}) E_i^{-T} J_i, \quad (25)$$

where \hat{H}_o and $\hat{\mu}$ include estimated value. The update rule for the uncertainty can be given as:

$$\dot{\hat{\Delta}}_i = -K_\Delta \mathbf{s}_i, \quad (26)$$

where K_Δ a user-defined diagonal matrix.

Lemma 2. *If $\mathbf{e}_i, \dot{\mathbf{e}}_i \in \mathcal{L}_\infty$ and $\mathbf{q}_i, \dot{\mathbf{q}}_i, \ddot{\mathbf{q}}_i \in \mathcal{L}_\infty$, then $\dot{\xi}_i$ is bounded as follows:*

$$\|\dot{\xi}_i\| \leq \rho_\xi \quad (27)$$

where ρ_ξ is a positive constant.

Proof. Consider the following compact sets:

$$\mathcal{D}_1 \triangleq \{(\mathbf{e}_i, \dot{\mathbf{e}}_i) \mid |\mathbf{e}_i|^2 + |\dot{\mathbf{e}}_i|^2 \leq \rho_1\}$$

$$\mathcal{D}_2 \triangleq \{(\mathbf{q}_i, \dot{\mathbf{q}}_i, \ddot{\mathbf{q}}_i) \mid |\mathbf{q}_i|^2 + |\dot{\mathbf{q}}_i|^2 + |\ddot{\mathbf{q}}_i|^2 \leq \rho_2\},$$

where ρ_1 and ρ_2 are positive constants. From (19), $\ddot{\mathbf{e}}_i$ can be rewritten as:

$$C^* \ddot{\mathbf{e}}_i = -K^* \dot{\mathbf{e}}_i + \tilde{D}_i \ddot{\mathbf{q}}_i + \tilde{C}_i \dot{\mathbf{q}}_i + \tilde{G}_i + \tilde{\Delta}_i \quad (28)$$

where \tilde{D}_i , \tilde{C}_i , \tilde{G}_i and $\tilde{\Delta}_i$ can be computed by (14) and (18). The right hand side of (28) can be seen as a function of \mathbf{e}_i , $\dot{\mathbf{e}}_i$, \mathbf{q}_i , $\dot{\mathbf{q}}_i$ and $\ddot{\mathbf{q}}_i$, which are all bounded. Therefore, we can say that $\ddot{\mathbf{e}}_i$ is bounded. Since $\ddot{\mathbf{e}}_i$ and $\dot{\mathbf{e}}_i$ are bounded, $\dot{\xi}_i$ is bounded on the compact set $\mathcal{D}_1 \times \mathcal{D}_2$. \square

In order to prove the stability of closed-loop dynamics, we use the following assumption.

Assumption 2. *The desired trajectory is bounded as:*

$$|\dot{\mathbf{q}}_i^d| + |\ddot{\mathbf{q}}_i^d| + |\dot{\mathbf{q}}_i^d| + |\ddot{\mathbf{q}}_i^d| \leq \rho,$$

where ρ is a positive constant.

Based on (21), the closed-loop dynamics is derived as:

$$D_i \dot{\mathbf{s}}_i + C_i \mathbf{s}_i + (K_s + \delta_i) \mathbf{s}_i = \tilde{D}_i \ddot{\mathbf{q}}_i^r + \tilde{C}_i \dot{\mathbf{q}}_i^r + \tilde{G}_i + \xi_i^f + \tilde{\Delta}_i, \quad (29)$$

where $\tilde{\Delta}_i$ is the uncertainty estimation error. Then, the following theorem can be given:

Theorem 1. *Consider the cooperative aerial manipulators with decoupled dynamics in (5) with the parameter estimator (17). Then, the sliding surface variable for i -th aerial manipulator, \mathbf{s}_i in (20), can be made arbitrarily small under the control input in (21). If, in addition, the state estimation error goes to zero, i.e., $\mathbf{e}_i \rightarrow 0$ or changes very slowly, then \mathbf{s}_i goes to zero asymptotically.*

Proof. See Appendix B. \square

IV. PATH PLANNING

In this section, we present the path generation algorithm based on task priority solution with activation function. Main objective of planning is to transport the unknown payload while the end effectors remain in the allowable flight envelope.

A. Allowable Payload for Each Aerial Manipulator

Here, we analyze the capability of the aerial manipulator with multi-DOF arm with respect to the position of the end effector. Unlike the results in [11], in this paper, we consider an allowable payload of the aerial manipulator regardless of the DOF of robotic arm. For this, let us consider the aerial robot and unknown payload first, in which the torque generated by the robotic arm will be combined later.

In order to operate the hexacopter, the control input τ_i in body frame Σ_b from first to sixth elements (i.e., $\tau_i(1 : 6)$) should be converted into the actuation command as:

$$\tau_i(1 : 6) = \Xi \mathbf{f}_i, \quad (30)$$

where $\mathbf{f}_i = [f_1, \dots, f_6]$ is the force of the each motor and $f_i = k_f \Omega_i$ with the thrust coefficient k_f and the desired speed of the rotor Ω_i . In addition, Ξ is the motor mapping matrix and can be defined as

$$\Xi = \begin{bmatrix} 0 & 0 & 0 & 0 & 0 & 0 \\ 0 & 0 & 0 & 0 & 0 & 0 \\ 1 & 1 & 1 & 1 & 1 & 1 \\ s_{30^\circ} r & r & s_{30^\circ} r & -s_{30^\circ} r & -r & -s_{30^\circ} r \\ -c_{30^\circ} r & 0 & c_{30^\circ} r & c_{30^\circ} r & 0 & -c_{30^\circ} r \\ -c_m & c_m & -c_m & c_m & -c_m & c_m \end{bmatrix}.$$

In our configuration, since the robotic arm swings with respect to the y axis in Σ_b , the lager torque can be applied to motor 1 or 6 as shown in Fig. 2. Therefore, when the gravitational force due to the maximum allowable payload $m_{o,i}^{\max}$ is acting on the end effector, the motor command can be calculated as:

$$k_f \Omega_{1,\max}^2 = \Xi^\dagger(1,:) \tau_i, \quad (31)$$

where $\Xi^\dagger(1,:)$ is the first row vector of Ξ^\dagger . By using (30), we can express the desired speed of motor 1 with the mass of a payload ($m_{o,i}^{\max}$) and the length between $\Sigma_{b,i}$ and $\Sigma_{c,i}$ in x direction (x_b^c) as:

$$6k_f \Omega_{1,\max}^2 = (m_b + m_{o,i}^{\max})g + \frac{\tau_\phi}{r_a} + \frac{6}{2\sqrt{3}r_a}(\tau_\theta + m_{o,i}^{\max}gx_b^c) + \frac{\tau_\psi}{c_m}, \quad (32)$$

where c_m is the ratio between the thrust and drag coefficient, g is the gravitational constant and r_a is the arm length of the hexacopter (i.e., $r_a = 0.2$ m in our configuration). $\Omega_{1,\max}$ is set to 9,200, because the possible range of revolutions per minute (RPM) of the motor is from 1,200 to 9,200. In addition, if the attitude error of the aerial manipulator is bounded by the maximum roll torque, the following equation is satisfied:

$$|K_\phi(\dot{\epsilon}_\phi + \Lambda_\phi e_\phi)| \leq K_\phi(\dot{\phi}_{\max} + \Lambda_\phi \phi_{\max}) := \tau_{\phi_{\max}}, \quad (33)$$

where K_ϕ and Λ_ϕ are user-defined gains in the ϕ direction. $\tau_{\theta_{\max}}$ and $\tau_{\psi_{\max}}$ can be expressed similarly. Here, we set

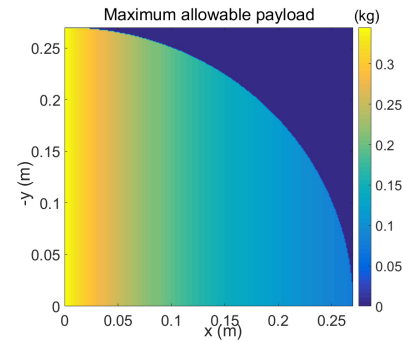


Fig. 4. Allowable payload with respect to the relative position of an object.

$\dot{\phi}_{\max} = 5$ deg and $\dot{\phi}_{\max} = 14$ deg/s. Finally, eq. (32) can be rewritten as:

$$m_{o,i}^{\max} = \left[r(6k_f \Omega_{1,\max}^2 - m_b g) - \frac{6}{2\sqrt{3}}\tau_{\theta_{\max}} - \frac{r}{c_m}\tau_{\psi_{\max}} - \tau_{\phi_{\max}} \right] / g(r_a + |x_b^c|). \quad (34)$$

From the user-defined gains used in the experiments, i.e., $K_\phi = 1.0$ and $\Lambda_\phi = 3.3$, the maximum allowable payload can be calculated by (34). Because eq. (34) does not consider the disturbances or efficiency of electric motor, we give 20 % additional margin on $m_{o,i}^{\max}$. As a result, the maximum allowable payload can vary from 0.15 kg to 0.36 kg with respect to the relative position of the object as shown in Fig. 4.

However, the result in Fig. 4 does not consider the effect of the robotic arm. Since the torque generated due to the movement of the robotic arm can reduce the allowable payload, we should compensate this torque to obtain the allowable payload for the aerial manipulator. If the torque generated by the robotic arm without a payload is $\tau_{arm,\theta}$ which is applied in the pitch direction of the hexacopter, then the maximum payload with this effect can be computed from (34) as

$$m_{o,i}^{\max} = m_{o,i}^{act} + \frac{6|\tau_{arm,\theta}|}{2\sqrt{3}g(r_a + |x_b^c|)} \quad (35)$$

where $m_{o,i}^{act}$ is the actual allowable payload of the hexacopter. For example, if the arm is in the straight forward position (i.e., $x_b^c = 0.27$ m) and $\tau_{arm,\theta} = 0.21$ Nm, the virtual payload due to the robotic arm is about 0.078 kg. Based on (35), the unilateral constraints in Fig. 4 can be determined by the total mass that is computed by adding the virtual mass due to the robotic arm to the estimated mass.

B. Trajectory Generation with Unilateral Constraints

The trajectory generation for each aerial manipulator consists of two layers : 1) kinematic coordination to generate the trajectory of each end effector and 2) motion generation with task priority solution. In the first layer, we compute the desired trajectory of each end effector (i.e., $\mathbf{p}_{e,i}^d$) from the desired trajectory of the object (i.e., $\mathbf{q}_{o,i}^d = [\mathbf{p}_o^d, \Phi_o^d]$). From the rigid grasping assumption, we can say that the relative distance from Σ_o and $\Sigma_{c,i}$, which we denote as \mathbf{r}_i , is constant.

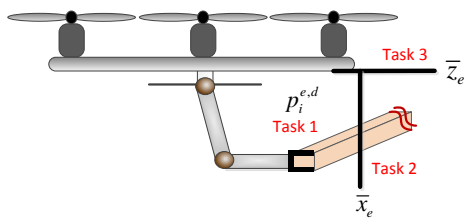


Fig. 5. Multiple factors for safe aerial transportation. (Task 1: trajectory for transportation, Task 2: unilateral constraints due to the allowable flight envelope, Task 3: unilateral constraints on z axis for the propeller protection.)

Then, the desired trajectory of the each end effector can be computed as:

$$\begin{aligned} \mathbf{p}_{e,i}^d &= \mathbf{p}_o^d + R_o(\Phi_o^d)\mathbf{r}_i \\ \dot{\mathbf{p}}_{e,i}^d &= \dot{\mathbf{p}}_o^d + S(\omega_o)\mathbf{r}_i, \end{aligned} \quad (36)$$

where R_o transforms a vector from frame Σ_o to frame Σ_I .

In the second layer, we generate the desired trajectory of each aerial manipulator (i.e., \mathbf{q}_i^d) to track the desired trajectory of the end effector (i.e., $\mathbf{p}_{e,i}^d$). The end effector of each aerial manipulator should remain in allowable region as shown in Fig. 4, while following the desired trajectory of the object. To achieve this goal, we use task priority solution which composes of three types of task as shown in Fig. 5.

The first priority task is the trajectory generation task for $\gamma_{i,1}$. To do so, let us consider the kinematic relationship of the end effector in which position of the end effector (i.e., $\mathbf{p}_{e,i}$) can be obtained by using the Cartesian position of the hexacopter (i.e., $\mathbf{p}_{b,i}$) and the position of the end effector with respect to $\Sigma_{b,i}$ (i.e., $\mathbf{p}_{e,i}^b$). The kinematic equation between $\mathbf{p}_{e,i}$ and $\mathbf{p}_{b,i}$ can be written as

$$\mathbf{p}_{e,i} = \mathbf{p}_{b,i} + R_{b,i}\mathbf{p}_{e,i}^b \quad (37)$$

where $R_{b,i}$ transforms a vector from frame $\Sigma_{b,i}$ to frame Σ_I , $\dot{\mathbf{p}}_{e,i}^b = J_\eta \dot{\mathbf{q}}_i$, and J_η is the Jacobian matrix. In addition, to control the attitude of the object, we should consider the orientation of each end effector. In our configuration, the pitch angle of the object and the pitch of the end effector should be aligned in the rigid grasping, so we set $\sum_{j=1}^n \eta_{i,j} = \theta_o$. Therefore, following the result of [39], we defined a new task variable for the i -th aerial manipulator as $\gamma_{i,1}^a := [\mathbf{p}_{e,i}; \cos(\sum_{j=1}^n \eta_{i,j})]^T$ in (9). Finally, we can establish a forward kinematic solution between $\dot{\gamma}_{i,1}^a$ and $\dot{\mathbf{q}}_i$ as:

$$\begin{aligned} \dot{\gamma}_{i,1}^a &= \begin{bmatrix} I_{3 \times 3} & -(R\mathbf{p}_{e,i}^b)^\wedge J_{\Phi_i} & R J_\eta \\ 0_{1 \times 3} & 0_{1 \times 3} & J_s \end{bmatrix} \dot{\mathbf{q}}_i \\ &:= T_{i,1} \dot{\nu}_{i,1} + \begin{bmatrix} B(\Phi_i) \\ 0_{1 \times 3} \end{bmatrix} \dot{\Phi}_i \end{aligned} \quad (38)$$

where $J_s = [-\sin(\sum_{j=1}^n \eta_{i,j}), \dots, -\sin(\sum_{j=1}^n \eta_{i,j})] \in \mathbb{R}^n$, J_{Φ_i} converts Φ_i into the angular velocity in $\Sigma_{b,i}$, and \wedge is the operator that converts a vector into a skew-symmetric matrix. Finally, the augmented desired position of the end effector (i.e., $\gamma_{i,1}$) is calculated as:

$$\dot{\gamma}_{i,1} = \dot{\gamma}_{i,1}^{a,d} + \kappa(\gamma_{i,1}^{a,d} - \gamma_{i,1}^a) - \begin{bmatrix} B(\Phi_i) \\ 0_{1 \times 3} \end{bmatrix} \dot{\Phi}_i \quad (39)$$

where $\gamma_{i,1}^{a,d}$ is the desired state of $\gamma_{i,1}^a$, $\kappa > 0$ is a diagonal gain matrix. To obtain $\nu_{i,1}$, we use inverse kinematics for redundant manipulators [39] as

$$\dot{\nu}_{i,1} = T_{i,1}^\dagger \dot{\gamma}_{i,1}. \quad (40)$$

However, the solution in (40) cannot guarantee the safe aerial transportation. To satisfy the unilateral constraint, we use task priority solution as described in [13]. Based on the allowable flight envelope, the end effector should not violate the unilateral constraints $\bar{x}_{e,i}$ which can vary depending on the estimated mass. The second task can be obtained based on (9) and (40) as:

$$\dot{\nu}_{i,2} = \dot{\nu}_{i,1} + h_1(T_{i,2}P_{i,1}^A)^\dagger(\dot{\gamma}_{i,2} - T_{i,2}\dot{\nu}_{i,1}) \quad (41)$$

Here, $T_{i,2}$ is the transformation matrix of the second task and $P_{i,1}^A = I_{(3+n) \times (3+n)} - T_{i,1}^\dagger T_{i,1}$. In (41), the discontinuity near boundary of $\bar{x}_{e,i}$ can be occur, which may cause degradation of tracking performance (See more detail in [12,13]). To resolve this problem, we use the smooth activation function in h_1 . The smooth activation function about boundary condition can be defined as

$$h_1 \begin{cases} 0 & x_e < \bar{x}_e - b_p \\ g\left(\frac{x_e - \bar{x}_e + b_p}{b_p}\right) & \bar{x}_e - b_p \leq x_e < \bar{x}_e \\ 1 & \bar{x}_e \leq x_e \end{cases}, \quad (42)$$

where b_p is a deactivation buffer and $g(a) = 6a^5 - 15a^4 + 10a^3$ is a quintic polynomial function which satisfies $g(0) = 0$ and $g(1) = 1$.

If the end effector exceeds the z axis limit (i.e., \bar{z}_e), the collision between the end effector and propellers can be occurred. For this reason, the third task considers the unilateral constraints on the z axis of the end effector. Following the same process as (41), $\dot{\nu}_{i,3}$ can be computed as:

$$\dot{\nu}_{i,3} = \dot{\nu}_{i,2} + h_2(T_{i,3}P_{i,2}^A)^\dagger(\dot{\gamma}_{i,3} - T_{i,3}\dot{\nu}_{i,2}), \quad (43)$$

where $T_{i,3}$ is the Jacobian matrix of the third task and $P_{i,2}^A = P_{i,1}^A - (T_{i,2}P_{i,1}^A)^\dagger T_{i,2}P_{i,1}^A$. The activation function h_2 can be computed same as (42). Finally, using $\dot{\nu}_{i,3}$, we reconstruct \mathbf{q}_i^d as

$$\mathbf{q}_i^d = [\nu_{i,3}(1 : 3), \phi_d, \theta_d, \psi_d, \nu_{i,3}(4 : 3 + n)]^T. \quad (44)$$

In the rigid grasping, yaw angles of object and aerial manipulators are aligned also, i.e., $\psi_i = \psi_o$, so ψ_d is set to be same with the desired yaw angle of the object.

Note that if the second or third task is near singularity, the damped solution can deform the original task such as $\dot{\nu}_{i,1}$. To resolve issue, the reverse priority approach can be applied [36]. However, in our configuration, since h_1 and h_2 are set to be zero near the corresponding singularity of the robotic arm, the task deformation does not affect the transportation performance. Therefore, although we use standard task priority solution in [35], there will be no deformation of the high priority task.

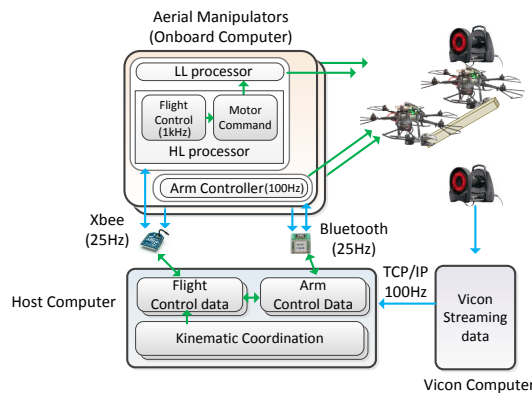


Fig. 6. Experimental setup.

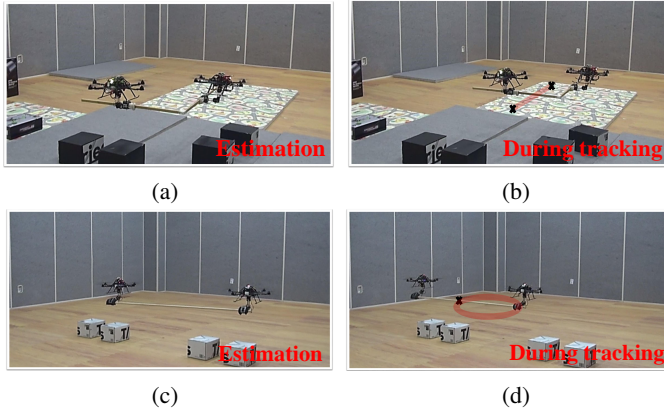


Fig. 7. Object trajectory tracking results. The red circles represent the desired trajectory of the object. (a) 'L' shape rod ($t=20$ sec). (b) 'L' shape rod ($t=50$ sec). (c) 'T' shape rod ($t=20$ sec). (d) 'T' shape rod ($t=50$ sec).

V. EXPERIMENT

In this section, we describe an experimental result with two custom-made aerial manipulators to carry an unknown payload. In experiment, we consider that each aerial manipulator consists of a hexacopter and a 2-DOF arm, so $n = 2$. In addition for simplicity, we have assumed that translational and angular velocities are small, which means that their product is negligible, i.e., $C(\mathbf{q}_i, \dot{\mathbf{q}}_i)\dot{\mathbf{q}}_i \approx 0$. Video of two experiments is available at http://icsl.snu.ac.kr/hbeam/TII_supplementary.mp4.

A. Experimental Setup

The platforms used in this paper are Ascending Technologies Firefly hexacopters. The robotic arms are customized with Dynamixel servomotors. The total length of each arm is 0.27 meter (i.e., $l_1 = l_2 = 0.135$). The total weight of the robotic arm is about 300 gram including the gripper before picking up the payload. The unknown payloads used in the experiment are a wooden rod of 'I' shape (1.8 meter, 280 gram) and a wooden rod of 'L' shape (0.9 meter for each side, 350 gram).

For experiment, we used Vicon, an indoor GPS system, which measures the position information with 100 Hz as shown in Fig. 6. The desired trajectory of the aerial manipulator and actual states of hexacopters and the joint angles

are transmitted to the hexacopter with Xbee at 25 Hz. The proposed estimator and controller run at 1 kHz in the onboard processor of the hexacopters. Arm control inputs are sent by Bluetooth at 25 Hz. Note that communication delay between multiple robots or packet drop has not been considered. The more details about time delay of networked robots can be found in [26].

The gain matrices $K_s = \text{diag}[9.5, 9.5, 5.5, 1.0, 1.0, 1.0, 0.5, 0.5]$, $\Lambda_i = \text{diag}[0.35, 0.35, 4.0, 3.2, 3.2, 3.2, 1.0, 1.0]$ and $K_\Delta = \text{diag}[2.0, 2.0, 3.0, 0.5, 0.5, 0.5, 0.0, 0.0]$ are selected. For the parameter update in (18), we set $\Gamma_1 = 0.05 \times I_{8 \times 8}$, $\Gamma_2 = 0.05 \times I_{8 \times 8}$, $C^* = 10 \times I_{8 \times 8}$ and $K^* = 20 \times I_{8 \times 8}$. The deactivation buffer is set to be $b_p = 0.05$ m.

In order to illustrate the performance in more detail, we prepare flight scenarios to transport the object. The desired trajectory of the object is set to be:

$$\begin{aligned} \mathbf{p}_o^d &= \left[\begin{array}{ccc} \frac{3}{10} \sin\left(\frac{\pi}{10}t\right) & \frac{3}{10} (\cos\left(\frac{\pi}{10}t\right) - 1) & 0.45 \end{array} \right] \\ \Phi_o^d &= \left[\begin{array}{ccc} 0 & 25 \sin\left(\frac{\pi}{40}t\right) - 25 & -10 \sin\left(\frac{\pi}{50}t\right) \end{array} \right], \end{aligned} \quad (45)$$

where the unit of Φ_o^d is degree.

In addition for the desired trajectory, since the behavior of the end-effector of the aerial manipulator is highly affected by the attitude of the hexacopter, the desired trajectory can be oscillated due to disturbances, which causes the performance degradation. To prevent this problem, we performed smoothing by applying the low-pass filter to the generated task solution $\dot{\mathbf{v}}_{i,3}$ as appeared in (43).

B. Experimental Result

We show results of autonomous transportation of two payloads. Fig. 7 shows snapshots taken during the planning and tracking experiment. For the rod of 'L' shape, cooperative aerial manipulators follow a straight line for the payload, while the rod of 'T' shape follows the trajectory in (45). When cooperative aerial manipulators take off with the payload before tracking the trajectory in (45), they cannot determine the allowable flight region because they do not know the mass of the payload. For this reason, at first, they estimate the unknown mass in hover flight during the first 22 seconds. Then, they follow the desired trajectory of the end effector during the next 40 seconds.

Figs. 8(a) and 8(c) present the trajectory tracking results of the common object. The blue solid line is the current state and the red dashed line is the desired state. As demonstrated in our experiment, the proposed algorithm shows satisfactory tracking performance when handling an unknown payload. The parameter estimation results are shown in Figs. 8(b) and 8(d). Our proposed algorithm with consensus shows more satisfactory estimation results, while the estimation result without consensus has clear error for the mass of the unknown common object. In addition, since the consensus algorithm makes the estimation result of two manipulators identical, two aerial manipulators can share the same flight envelope, which results in the synchronized motion of the robotic arms.

Fig. 9 shows time histories of \mathbf{q}_i and $\dot{\mathbf{q}}_i$ to track the generated trajectory in (45) by using the task priority solution in (43). The magenta dashed lines in the bottom figures of Fig.

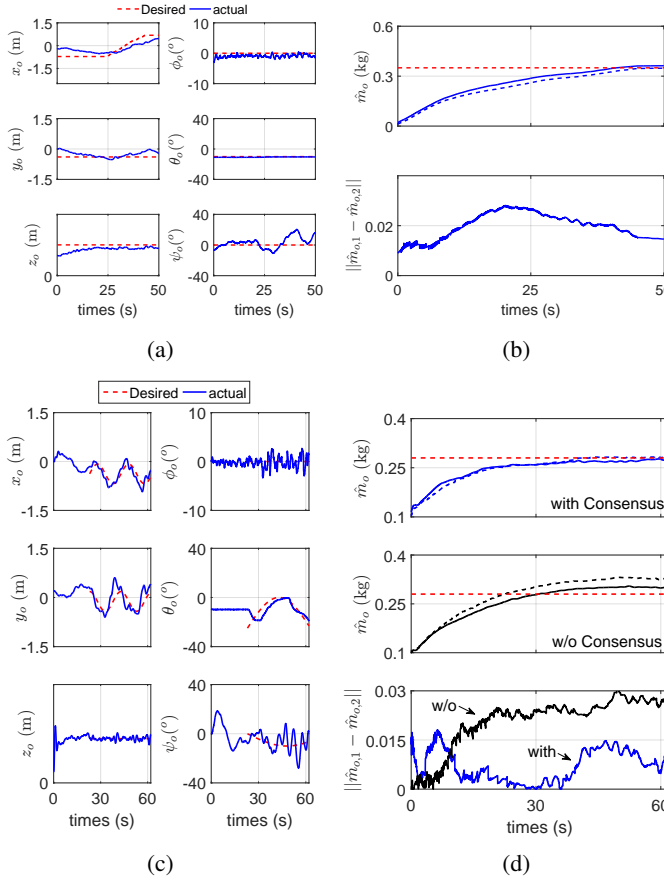


Fig. 8. Estimation and tracking results (a-b: ‘L’ Shape, c-d: ‘I’ Shape). (a) Time histories of q_o . (b) Parameter estimation. (c) Time histories of q_o . (d) Parameter estimation with or without consensus.

9(c) and Fig. 9(f) mean the unilateral constraints for the end effector to satisfy the allowable flight envelope. Although the constraints $\bar{x}_{e,i}$ can vary depending on the estimated mass, $\bar{x}_{e,1}$ and $\bar{x}_{e,2}$ are set to be almost the same thanks to the consensus algorithm. Based on our proposed synthesis, the aerial manipulators can transport the unknown payload while satisfying the unilateral constraints in $\bar{x}_{e,i}$ and $\bar{z}_{e,i}$.

VI. CONCLUSION

This paper presented the planning and control synthesis for cooperative aerial manipulators to cope with an unknown payload. The unknown parameter of the common payload was estimated using on-line parameter estimation algorithm. The adaptive sliding mode controller was designed to control each aerial manipulator with a 2-DOF robotic arm. To generate the path for transporting an object, the desired trajectory of the end effector was generated by using kinematic coordination. The task priority solution with unilateral constraints was used to track the trajectory of the end effector. In the experimental result, we showed a successful flight experiment using multiple custom-made aerial manipulators, remaining in the flight envelope computed based on the analysis of the maximum rotor speed.

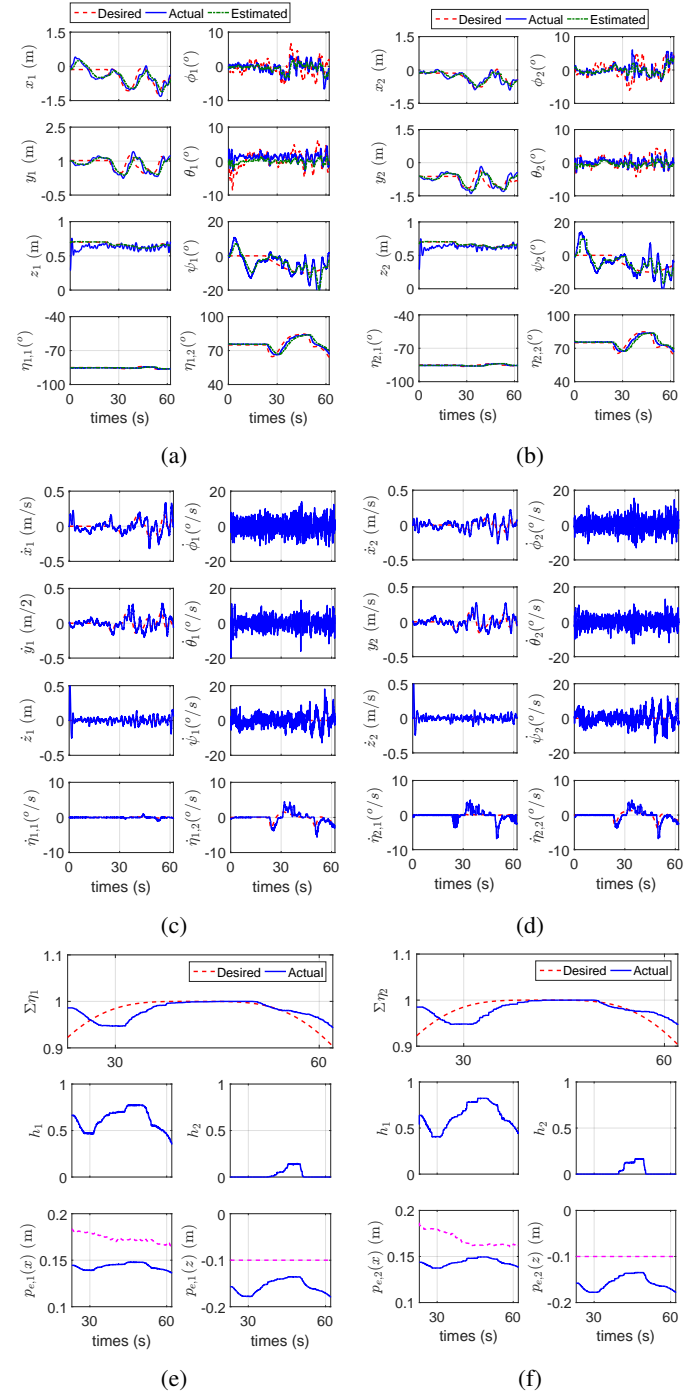


Fig. 9. Time histories of q_i and \dot{q}_i . (a) Time histories of q_1 . (b) Time histories of q_2 . (c) Time histories of \dot{q}_1 . (d) Time histories of \dot{q}_2 . (e) Constraints for q_1 . (f) Constraints for q_2 .

APPENDIX A. PROOF OF LEMMA 1

In order to prove the convergence of the error dynamics (19), we first define the Lyapunov candidate function for all agents as:

$$V = \sum_{i=1}^{N_m} V_i, \quad (46)$$

where

$$V_i = \frac{1}{2} \mathbf{e}_i^T C^* \mathbf{e}_i + \frac{1}{2\Gamma_1} \tilde{m}_{o,i}^2, \quad (47)$$

where $\tilde{m}_{o,i} = \hat{m}_{o,i} - m_{o,i}$ is the estimation error. The time derivative of V_i is given as:

$$\begin{aligned} \dot{V}_i &= \mathbf{e}_i^T C^* \dot{\mathbf{e}}_i + \frac{1}{\Gamma_1} \tilde{m}_{o,i} \dot{\hat{m}}_{o,i} \\ &= -\mathbf{e}_i^T K^* \mathbf{e}_i - \tilde{m}_{o,i} \mathbf{e}_i^T (H_1 \ddot{\mathbf{q}}_i + H_2 \dot{\mathbf{q}}_i + H_3) + \frac{1}{\Gamma_1} \tilde{m}_{o,i} \dot{\hat{m}}_{o,i}, \end{aligned} \quad (48)$$

where $\dot{\hat{m}}_{o,i} = \dot{\tilde{m}}_{o,i}$. Now, substituting the update rule (18) into (48), \dot{V}_i can be rewritten as:

$$\dot{V}_i = -\mathbf{e}_i^T K^* \mathbf{e}_i + \frac{\Gamma_2}{\Gamma_1} \tilde{m}_{o,i} \sum_{j=1}^{N_m} (\tilde{m}_{o,j} - \tilde{m}_{o,i}), \quad (49)$$

where $(\tilde{m}_{o,j} - \tilde{m}_{o,i}) = (\hat{m}_{o,j} - \hat{m}_{o,i})$. Using the fact that

$$\sum_{i=1}^{N_m} \tilde{m}_{o,i} \sum_{j=1}^{N_m} (\tilde{m}_{o,j} - \tilde{m}_{o,i}) = -\frac{1}{2} \sum_{i=1}^{N_m} \sum_{j=1}^{N_m} (\tilde{m}_{o,j} - \tilde{m}_{o,i})^2,$$

eq. (46) can be rewritten as:

$$\dot{V} = -\sum_{i=1}^{N_m} \mathbf{e}_i^T K^* \mathbf{e}_i - \frac{\Gamma_2}{2\Gamma_1} \sum_{i=1}^{N_m} \sum_{j=1}^{N_m} (\tilde{m}_{o,j} - \tilde{m}_{o,i})^2 \leq 0.$$

This proves the boundedness of $\mathbf{e}_i, \tilde{m}_{o,i}$. We can also say that $\dot{\mathbf{e}}_i$ and $\dot{\tilde{m}}_{o,i}$ are bounded, because $\ddot{\mathbf{q}}_i$ and $\ddot{\tilde{\mathbf{q}}}_i$ are bounded in (18) and (19). Then \ddot{V} is also bounded, which guarantees that the state estimation error (i.e., \mathbf{e}_i) and consensus error (i.e., $|\hat{m}_{o,j} - \hat{m}_{o,i}|$ when $i \neq j$) go to 0 asymptotically by applying Barbalat's lemma.

APPENDIX B. PROOF OF THEOREM 1

The stability of the closed dynamics in (29) can be achieved by using the following Lyapunov candidate function:

$$\begin{aligned} V_i^c &= \frac{1}{2} \mathbf{s}_i^T \hat{D}_i \mathbf{s}_i + \frac{1}{2} \tilde{\Delta}_i^T K_\Delta^{-1} \tilde{\Delta}_i + \frac{1}{2} \chi_i^T \chi_i \\ &\leq \frac{1}{2} \lambda_{\max}(\hat{D}_i) \|\mathbf{s}_i\|^2 + \frac{\|K_\Delta^{-1}\|}{2} \|\tilde{\Delta}_i\|^2 + \frac{1}{2} \|\chi_i\|^2 := \bar{V}_i^c \end{aligned} \quad (50)$$

where $\chi_i = \xi_i^f - \xi_i$. The time derivative of V_i^c can be obtained as:

$$\begin{aligned} \dot{V}_i^c &= \mathbf{s}_i^T D_i \dot{\mathbf{s}}_i + \frac{1}{2} \mathbf{s}_i^T \dot{D}_i \mathbf{s}_i + \mathbf{s}_i^T \tilde{D}_i \dot{\mathbf{s}}_i + \frac{1}{2} \mathbf{s}_i^T \dot{\tilde{D}}_i \mathbf{s}_i \\ &\quad + \tilde{\Delta}_i^T K_\Delta^{-1} \dot{\tilde{\Delta}}_i + \chi_i^T \dot{\chi}_i, \end{aligned} \quad (51)$$

where $\tilde{D}_i = \hat{D}_i - D_i$ and $\tilde{\Delta}_i = \hat{\Delta}_i - \Delta_i$. From (19), we can obtain $\tilde{G}_i = -\xi_i - \tilde{D}_i \ddot{\mathbf{q}}_i - \tilde{C}_i \dot{\mathbf{q}}_i$. Then we can rewrite (51) as:

$$\begin{aligned} \dot{V}_i^c &= \mathbf{s}_i^T [-C_i \mathbf{s}_i - (K_s + \delta_i) \mathbf{s}_i + \tilde{D}_i \ddot{\mathbf{q}}_i^r - \tilde{D}_i \ddot{\mathbf{q}}_i + \tilde{C}_i \dot{\mathbf{q}}_i^r \\ &\quad - \tilde{C}_i \dot{\mathbf{q}}_i + \xi_i^f - \xi_i + \tilde{\Delta}_i] + \mathbf{s}_i^T \tilde{D}_i \dot{\mathbf{s}}_i + \frac{1}{2} \mathbf{s}_i^T \dot{D}_i \mathbf{s}_i \\ &\quad + \frac{1}{2} \mathbf{s}_i^T \dot{\tilde{D}}_i \mathbf{s}_i + \tilde{\Delta}_i^T K_\Delta^{-1} \dot{\tilde{\Delta}}_i + \chi_i^T \dot{\chi}_i. \end{aligned} \quad (52)$$

In this case, since $\frac{1}{2} \mathbf{s}_i^T (\dot{\hat{D}}_i - 2\hat{C}_i) \mathbf{s}_i - \mathbf{s}_i^T \delta_i \mathbf{s}_i = 0$, from (25) and (26), we can simplify \dot{V}_i^c as:

$$\begin{aligned} \dot{V}_i^c &= -\mathbf{s}_i^T \chi_i - \mathbf{s}_i^T K_s \mathbf{s}_i - \frac{1}{\alpha} \chi_i^T \chi_i - \chi_i^T \dot{\xi}_i, \\ &\leq -\lambda_{\min}(K_s) \|\mathbf{s}_i\|^2 - \frac{1}{\alpha} \|\chi_i\|^2 + \|\mathbf{s}_i\| \|\chi_i\| + \|\chi_i\| \|\dot{\xi}_i\| \end{aligned} \quad (53)$$

In the derivation, we use the fact that $\dot{\chi}_i := \xi_i^f - \xi_i = \frac{\chi_i}{\alpha} - \dot{\xi}_i$. $\lambda_{\min}(K_s)$ is smallest eigenvalue of the matrix K_s . By using Lemma 2 and Young's inequality, i.e., $\mathbf{a}^T \mathbf{b} \leq \|\mathbf{a}\| \|\mathbf{b}\| \leq \frac{1}{2} \|\mathbf{a}\|^2 + \frac{1}{2} \|\mathbf{b}\|^2$ for two vectors \mathbf{a} and \mathbf{b} , the eq. (53) is rewritten as:

$$\begin{aligned} \dot{V}_i^c &\leq -\kappa_1 \|\chi_i\|^2 - \kappa_2 \|\mathbf{s}_i\|^2 + 1 \\ &\leq -2\beta \bar{V}_i^c + \beta \|K_\Delta^{-1}\| \|\tilde{\Delta}_i\|^2 + 1 \end{aligned} \quad (54)$$

where $\kappa_1 := (\frac{1}{\alpha} - \rho_\xi^2) > 0$, $\kappa_2 := (\lambda_{\min}(K_s) - \frac{1}{2}) > 0$ and $0 < \beta < \min(\kappa_1, \kappa_2 / \lambda_{\max}(\hat{D}_i))$.

Finally, assumming that disturbance $\|K_\Delta^{-1}\| \|\tilde{\Delta}_i\|$ is bounded, we can prove that V_i^c is finally bounded as same as [11]. According to the definition of uniformly ultimately bounded (UUB) property and the Lypunov's theorem [40], all the error signals of the overall closed-loop system (i.e., \mathbf{s}_i , $\tilde{\Delta}_i$ and χ_i) are UUB. In this case, \mathbf{s}_i can be made arbitrarily small by adjusting the upper bound of V_i^c . In addition, with $(\mathbf{e}_i, \dot{\mathbf{e}}_i) \rightarrow 0$ as shown in Lemma 1, we have asymptotic convergence of $\mathbf{s}_i \rightarrow 0$, because $\chi_i \rightarrow 0$ in (53).

REFERENCES

- [1] H. Lee and H. J. Kim, "Trajectory tracking control of multirotors from modelling to experiments: A survey," *Int. J. Control Autom.*, vol. 15, no. 1, pp. 281–292, 2017.
- [2] F. Caccavale, G. Giglio, G. Muscio, and F. Pierri, "Cooperative impedance control for multiple uavs with a robotic arm," in *Proc. IEEE/RSJ Int. Conf. Intell. Robot. Syst. (IROS)*, Sep. 2015, pp. 2366–2371.
- [3] G. Muscio, F. Pierri, M. Trujillo, E. Cataldi, G. Giglio, G. Antonelli, F. Caccavale, A. Viguria, S. Chiaverini, and A. Ollero, "Experiments on coordinated motion of aerial robotic manipulators," in *Proc. IEEE Int. Conf. Robot. Autom. (ICRA)*, May 2016, pp. 1224–1229.
- [4] D. Mellinger, M. Shomin, N. Michael, and V. Kumar, "Cooperative grasping and transport using multiple quadrotors," in *Distributed autonomous robotic systems*. Springer, 2013, pp. 545–558.
- [5] J. Fink, N. Michael, S. Kim, and V. Kumar, "Planning and control for cooperative manipulation and transportation with aerial robots," *Int. J. Robot. Res.*, vol. 30, no. 3, pp. 324–334, 2011.
- [6] H. Lee, H. Kim, and H. J. Kim, "Planning and control for collision-free cooperative aerial transportation," *IEEE Trans. Autom. Sci. Eng.*, vol. PP, pp. 1–13, 2016.
- [7] H. Yang and D. Lee, "Hierarchical cooperative control framework of multiple quadrotor-manipulator systems," in *Proc. IEEE Int. Conf. Robot. Autom. (ICRA)*, May 2015, pp. 4656–4662.
- [8] D. Devaurs, T. Siméon, and J. Cortés, "Optimal path planning in complex cost spaces with sampling-based algorithms," *IEEE Trans. Autom. Sci. Eng.*, vol. 13, no. 2, pp. 415–424, Apr. 2016.
- [9] S. Erhart and S. Hirche, "Model and analysis of the interaction dynamics in cooperative manipulation tasks," *IEEE Trans. Robot.*, vol. 32, no. 3, pp. 672–683, Jun. 2016.
- [10] A. Franchi, A. Petitti, and A. Rizzo, "Decentralized parameter estimation and observation for cooperative mobile manipulation of an unknown load using noisy measurements," in *Proc. IEEE Int. Conf. Robot. Autom. (ICRA)*, May 2015, pp. 5517–5522.
- [11] H. Lee and H. J. Kim, "Estimation, control, and planning for autonomous aerial transportation," *IEEE Trans. Ind. Electron.*, vol. 64, no. 4, pp. 3369–3379, Apr. 2017.
- [12] N. Mansard, O. Khatib, and A. Kheddar, "A unified approach to integrate unilateral constraints in the stack of tasks," *IEEE Trans. Robot.*, vol. 25, no. 3, pp. 670–685, Jun. 2009.

- [13] F. Flacco and A. De Luca, "Unilateral constraints in the reverse priority redundancy resolution method," in *Proc. IEEE/RSJ Int. Conf. Intell. Robot. Syst. (IROS)*, Sep. 2015, pp. 2564–2571.
- [14] T. Yoshikawa and X.-Z. Zheng, "Coordinated dynamic hybrid position/force control for multiple robot manipulators handling one constrained object," *Int. J. Robot. Res.*, vol. 12, no. 3, pp. 219–230, 1993.
- [15] D. Sieber, F. Deroo, and S. Hirche, "Formation-based approach for multi-robot cooperative manipulation based on optimal control design," in *Proc. IEEE/RSJ Int. Conf. Intell. Robot. Syst. (IROS)*, Nov. 2013, pp. 5227–5233.
- [16] P. Chiacchio, S. Chiaverini, and B. Siciliano, "Direct and inverse kinematics for coordinated motion tasks of a two-manipulator system," *J. Dyn. Syst. T. ASME*, vol. 118, no. 4, pp. 691–697, 1996.
- [17] F. Caccavale, P. Chiacchio, and S. Chiaverini, "Task-space regulation of cooperative manipulators," *Automatica*, vol. 36, no. 6, pp. 879–887, 2000.
- [18] Y. Kume, Y. Hirata, and K. Kosuge, "Coordinated motion control of multiple mobile manipulators handling a single object without using force/torque sensors," in *Proc. IEEE/RSJ Int. Conf. Intell. Robot. Syst. (IROS)*, Oct. 2007, pp. 4077–4082.
- [19] J. J. Craig, P. Hsu, and S. S. Sastry, "Adaptive control of mechanical manipulators," *Int. J. Robot. Res.*, vol. 6, no. 2, pp. 16–28, 1987.
- [20] W. Dong, "On trajectory and force tracking control of constrained mobile manipulators with parameter uncertainty," *Automatica*, vol. 38, no. 9, pp. 1475–1484, 2002.
- [21] B. Xiao, S. Yin, and O. Kaynak, "Tracking control of robotic manipulators with uncertain kinematics and dynamics," *IEEE Trans. Ind. Electron.*, vol. 63, no. 10, pp. 6439–6449, Oct. 2016.
- [22] F. Aghili, "Adaptive control of manipulators forming closed kinematic chain with inaccurate kinematic model," *IEEE/ASME Trans. Mechatronics*, vol. 18, no. 5, pp. 1544–1554, Oct. 2013.
- [23] R. Monfaredi, S. M. Rezaei, and A. Talebi, "A new observer-based adaptive controller for cooperative handling of an unknown object," *Robotica*, vol. 34, no. 07, pp. 1437–1463, 2016.
- [24] H. Kawasaki, S. Ueki, and S. Ito, "Decentralized adaptive coordinated control of multiple robot arms without using a force sensor," *Automatica*, vol. 42, no. 3, pp. 481–488, 2006.
- [25] X. Zhao, C. Ma, X. Xing, and X. Zheng, "A stochastic sampling consensus protocol of networked euler-lagrange systems with application to two-link manipulator," *IEEE Trans. Ind. Informat.*, vol. 11, no. 4, pp. 907–914, Aug. 2015.
- [26] X. Liang, H. Wang, Y. H. Liu, W. Chen, G. Hu, and J. Zhao, "Adaptive task-space cooperative tracking control of networked robotic manipulators without task-space velocity measurements," *IEEE Trans. Cybern.*, vol. 46, no. 10, pp. 2386–2398, Oct. 2016.
- [27] D. Mellinger, Q. Lindsey, M. Shomin, and V. Kumar, "Design, modeling, estimation and control for aerial grasping and manipulation," in *Proc. IEEE/RSJ Int. Conf. Intell. Robot. Syst. (IROS)*, Sept. 2011, pp. 2668–2673.
- [28] H. Liu, X. Wang, and Y. Zhong, "Quaternion-based robust attitude control for uncertain robotic quadrotors," *IEEE Trans. Ind. Informat.*, vol. 11, no. 2, pp. 406–415, Apr. 2015.
- [29] P. E. Pounds, D. R. Bersak, and A. M. Dollar, "Stability of small-scale uav helicopters and quadrotors with added payload mass under pid control," *Auton. Robots*, vol. 33, no. 1-2, pp. 129–142, 2012.
- [30] F. Morbidi, R. Cano, and D. Lara, "Minimum-energy path generation for a quadrotor uav," in *Proc. IEEE Int. Conf. Robot. Autom. (ICRA)*, May 2016, pp. 1492–1498.
- [31] R. Rossi, A. Santamaría-Navarro, J. Andrade-Cetto, and P. Rocco, "Trajectory generation for unmanned aerial manipulators through quadratic programming," *IEEE Robot. Autom. Lett.*, vol. 2, no. 2, pp. 389–396, Apr. 2017.
- [32] M. Korayem, M. Irani, A. Charesaz, A. Korayem, and A. Hashemi, "Trajectory planning of mobile manipulators using dynamic programming approach," *Robotica*, vol. 31, no. 04, pp. 643–656, 2013.
- [33] S. Erhart and S. Hirche, "Internal force analysis and load distribution for cooperative multi-robot manipulation," *IEEE Trans. Robot.*, vol. 31, no. 5, pp. 1238–1243, Oct. 2015.
- [34] B. Zhao, B. Xian, Y. Zhang, and X. Zhang, "Nonlinear robust adaptive tracking control of a quadrotor uav via immersion and invariance methodology," *IEEE Trans. Ind. Electron.*, vol. 62, no. 5, pp. 2891–2902, May 2015.
- [35] B. Siciliano and J.-J. E. Slotine, "A general framework for managing multiple tasks in highly redundant robotic systems," in *Int. Conf. Adv. Robot.*, 1991, pp. 1211–1216.
- [36] F. Flacco and A. De Luca, "A reverse priority approach to multi-task control of redundant robots," in *Proc. IEEE/RSJ Int. Conf. Intell. Robot. Syst. (IROS)*, Sep. 2014, pp. 2421–2427.
- [37] A. Colomé and C. Torras, "Closed-loop inverse kinematics for redundant robots: Comparative assessment and two enhancements," *IEEE/ASME Trans. Mechatronics*, vol. 20, no. 2, pp. 944–955, Apr. 2015.
- [38] J. J. Lim, H. Pirsiavash, and A. Torralba, "Parsing ikea objects: Fine pose estimation," in *Proc. IEEE Int. Conf. Comp. Vis. (ICCV)*, Dec. 2013, pp. 2992–2999.
- [39] Y. Nakamura, H. Hanafusa, and T. Yoshikawa, "Task-priority based redundancy control of robot manipulators," *Int. J. Robot. Res.*, vol. 6, no. 2, pp. 3–15, 1987.
- [40] H. K. Khalil, *Nonlinear Systems*. Prentice-Hall, New Jersey, 1996.



Hyeonbeom Lee received the B.S. degree in Mechanical and Control Engineering from Handong Global University in 2011, and the M.S. degree in Mechanical and Aerospace Engineering from Seoul National University in 2013. He is currently pursuing the Ph.D. degree in the Department of Mechanical and Aerospace Engineering at Seoul National University. His research interests include cooperative aerial manipulation and motion planning of aerial robots.



H. Jin Kim (S'98-M'02) received the B.S. degree from Korea Advanced Institute of Technology (KAIST) in 1995, and the M.S. and Ph.D. degrees in Mechanical Engineering from University of California, Berkeley (UC Berkeley) in 1999 and 2001, respectively. From 2002 to 2004, she was a Postdoctoral Researcher in Electrical Engineering and Computer Science (EECS), UC Berkeley. In September 2004, she joined the Department of Mechanical and Aerospace Engineering at Seoul National University, Seoul, Korea, as an Assistant Professor where she is currently a Professor. Her research interests include intelligent control of robotic systems and motion planning.